ELSEVIER

Geoderma 78 (1997) 207–236

GEODERMA

Soil development along an elevational transect in the western Sierra Nevada, California

R.A. Dahlgren [a,*], J.L. Boettinger [b], G.L. Huntington [a], R.G. Amundson [c]

[a] *Department of Land, Air and Water Resources, Hoagland 151, University of California, Davis, CA 95616, USA*

[b] *Department of Plants, Soils, and Biometeorology, Utah State University, Logan, UT 84322, USA*

[c] *E.S.P.M. Ecosystem Sciences Division, University of California, Berkeley, CA 94720, USA*

Received 15 August 1996; accepted 25 March 1997

Abstract

Soil development along an elevational transect on the western slopes of the central Sierra Nevada was investigated to assess the effects of climate on soil properties and processes. The transect of seven soils formed in granitic residuum spans elevations from 198 to 2865 m with mean annual temperature and precipitation differences of 13°C (3.9–16.7) and 94 cm (33–127), respectively. Soil pH decreased by about two units and base saturation decreased from 90 to 10% with increasing elevation. Concentrations of organic C in the solum increased with elevation, with the largest single increase occurring between the oak woodland (5–6 kg C/m^2) and mixed-conifer sites (10–15 kg C/m^2). Clay mineralogy showed a general trend of desilication and hydroxy-Al interlayering of 2 : 1 layer silicates with increasing elevation. The degree of chemical weathering, based on clay and secondary Fe oxide concentrations in the solum, showed a maximum (clay = 536 kg/m^2 and Fe oxides = 24 kg/m^2) at mid-elevations having intermediate levels of precipitation and temperature. While some soil properties show a continuous progression (e.g., organic carbon, base saturation, clay mineralogy) with elevation, other properties (e.g., pH, soil color, clay and secondary Fe oxide concentrations) show a pronounced change (threshold-type step) over a short distance at about 1600 m. The explanation for the abrupt nature of this shift is

* Corresponding author. Fax: +1 (916) 752-1552; E-mail: radahlgren@ucdavis.edu

PII S0016-7061(97)00034-7

not known; however, it coincides with the approximate elevation of the present-day average effective winter snow-line. © 1997 Elsevier Science B.V.

Keywords: clay mineralogy; climate; organic matter; soil acidity; soil genesis; weathering

1. Introduction

Climatic factors, particularly precipitation and temperature, dramatically influence soil properties by affecting types and rates of chemical, biological, and physical processes. Quantitative studies of pedogenesis have been used for nearly 70 years to examine the effects of climatic factors on soil properties and processes (Jenny, 1928, 1941, 1980). There is currently a renewed interest in using such studies for predicting possible biogeochemical feedback mechanisms in response to global climate change associated with anthropogenic emissions of CO_2.

Soils play a major role in the global biogeochemical cycle including storage of nutrients and carbon. At least twice as much C is stored in soils (ca. 1500×10^{15} g C) as in the atmosphere (ca. 720×10^{15} g C) or the vegetation (ca. 560×10^{15} g C) (Schlesinger, 1991). Carbon dioxide is converted to bicarbonate and nutrients are released during carbonic acid weathering of silicate minerals, thus contributing to both carbon and nutrient cycling. Climate change can have significant impacts on the global biogeochemical cycle by altering the type and rate of soil processes and the resulting soil properties. Climate directly influences vegetation type and quantity, weathering rates, and leaching intensity resulting in feedbacks to soil properties such as amount and quality of soil organic matter, clay content and mineralogy, cation exchange capacity, and base saturation.

Elevational transects are often used to obtain large variations in temperature and precipitation over relatively short distances. Soils along such transects can serve as spatial analogues to soils affected by climate change, allowing assessment of both the types and rates of change in soil processes and properties. The western slope of the central Sierra Nevada of California provides a nearly ideal opportunity for quantitatively examining the effect of climate on soil properties: the granitic parent material is relatively consistent in composition over an elevational transect subject to orographic climate effects. Several landmark studies of climatic effects on soil processes and properties focused on this area, particularly with respect to litter decomposition rates (Jenny et al., 1949; Trumbore et al., 1996) and clay, organic C, and N concentrations (Huntington, 1954; Harradine and Jenny, 1958); however, there are no complete studies of soil development along this elevational transect.

The purpose of this paper is to document the soil chemical, physical, and mineralogical properties and pedogenic processes along an elevational transect on the western slopes of the central Sierra Nevada, California. Representative pedons of seven soil series, each typifying the dominant soils that occur within a given elevational zone, were examined. Since all of the soils formed from similar granitic parent material, the trends of increasing precipitation and decreasing temperature with increasing elevation permit study of the effects of various climatic combinations on soil development. The transect

spans a range of 2650 m in elevation, 13°C in mean annual air temperature, and 94 cm in precipitation.

2. Materials and methods

2.1. Study area

This study examined an elevational transect of seven well-drained soils on the western slope of the Sierra Nevada in central California (Fig. 1). Each of the soils is representative of extensive areas of similar soils mapped in the central and southern

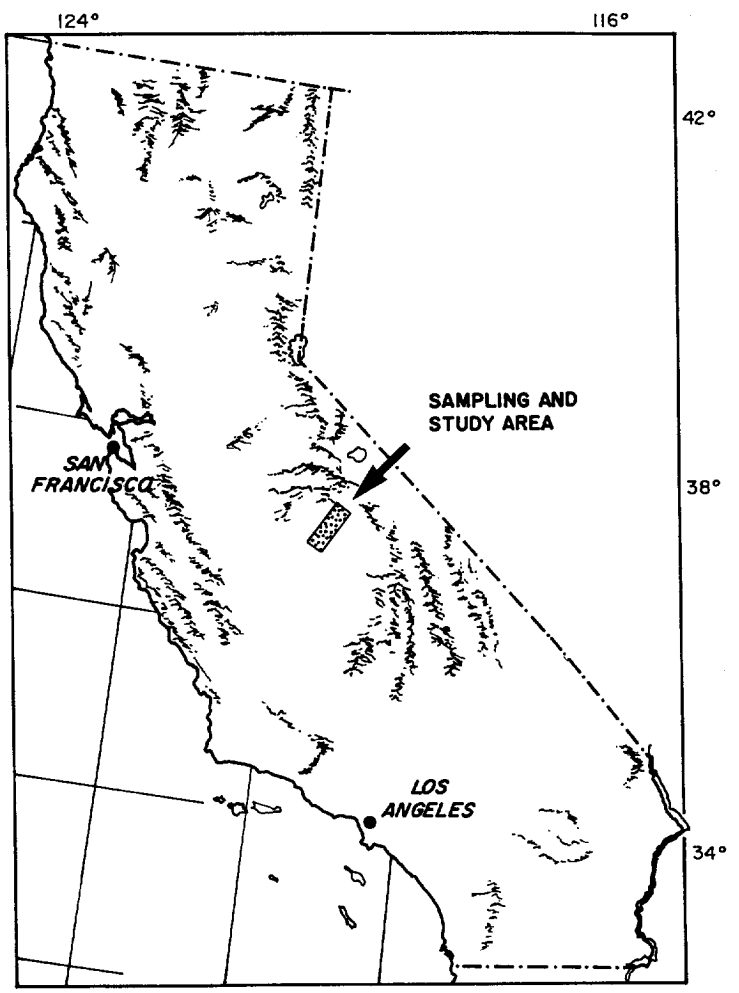

Fig. 1. Location of the elevational transect on the western slopes of the Sierra Nevada, California.

Sierra Nevada (USDA California Forest and Range Experiment Station, 1955–1960; USDA Soil Conservation Service, 1968; USDA Forest Service, 1986; Huntington and Akeson, 1987). The transect spans a distance of 64 km from near Millerton Lake (elevation 198 m) to Kaiser Pass (elevation 2865 m) (Table 1). Within the context of the state factor approach to soil formation (Jenny, 1941), we have attempted to keep all factors as constant as possible along the elevational transect, with the exception of climate.

All soils formed in residuum weathered from granitic bedrock (non-glaciated), which varies somewhat in chemical and mineralogical composition between granodiorite and tonalite (Table 1). All soil sampling sites have a southerly aspect and are situated on knoll-crest geomorphic landscape positions with slopes ranging from 9 to 15%. There was no evidence of accelerated erosion at any of the sampling sites although natural rates of erosion may vary with the amount of ground cover, frequency of ground cover disturbance, and the amount, intensity and form of precipitation.

Variations in climate and the resulting vegetation are the major differences between the seven study sites (Table 1). Climate at all sites is characterized as Mediterranean with cool to cold, wet winters and warm to hot, dry summers. With increasing elevation along the transect, mean annual air temperature decreases from 16.7° to 3.9°C (4.9°C per 1000 m) (Harradine and Jenny, 1958) and mean annual precipitation increases from 33 to 127 cm ($\sim$ 34 cm per 1000 m) (Steve Guilforyle, pers. commun., Southern Cal Edison Power, 1995). Soil temperature regimes, as defined in Soil Taxonomy (Soil Survey Staff, 1994), range through the progression thermic, mesic, frigid, and cryic with increasing elevation. The soil moisture regime (Soil Survey Staff, 1994) is xeric at lower elevations and is probably udic above approximately 2100 m. The average effective winter snow-line in this portion of the Sierra Nevada is at 1594 m (California Department of Water Resources, 1952–62). Above this elevation the majority of the precipitation falls as snow, while at lower elevations rain is the primary form of precipitation or the snow melts between winter storms. Four distinct vegetation zones exist: oak woodlands ($<$ 1008 m), oak/mixed-conifer forest (1008–1580 m), mixed-conifer forest (1580–2626 m), and subalpine mixed-conifer forest (2626–3200 m) (Table 1). Since there are no biotic barriers occurring along the elevational transect, the differences in vegetation are a function of climatic factors.

All pedons sampled in this study were genetically consistent with no evidence of natural or human perturbations. Within each elevational zone related to a particular soil the morphological features are remarkably consistent. We are inclined to believe that surface removal of soil by erosion and subsoil weathering approximately balance, and as a result, the profiles are in a quasi steady-state. Thus, we assume that the time factor is constant for all soils along the transect.

2.2. Methods

Soils were described in the field and samples were collected from each genetic horizon for laboratory analyses (Soil Survey Staff, 1981, 1984). Soil samples were air-dried, gently crushed, and passed through a 2-mm sieve to remove coarse fragments. The air-dried, $<$ 2-mm soil was used for the following analyses unless otherwise noted.

Table 1
Soil classification and description of soil-forming factors for the seven pedons composing the elevational transect on the western slopes of the Sierra Nevada

Soil series	Site elevation/Series range [a] (m)	Parent material (Formation name) [b]	Dominant vegetation at sampling site [c]	Temp. (°C) [d]	Precipitation (cm)	Classification
Chiquito [e]	2865/2626–3259	Granodiorite (Mt. Givens)	*Pinus contorta murrayana*; *Pinus monticola*; *Lupinus* species	3.9	127	Sandy-skeletal, mixed; Entic Cryumbrept
Sirretta	2195/2050–2626	Granodiorite (Dinkey Creek)	*Pinus jeffreyi*; *Abies magnifica*; *Abies concolor*	7.2	108	Sandy-skeletal, mixed, frigid; Dystric Xerorthent [f]
Shaver	1800/1688–2050	Granodiorite (Dinkey Creek)	*Abies concolor*; *Pinus lambertiana*; *Pinus ponderosa*; *Calocedrus decurrens*	9.1	101	Sandy, mixed, mesic; Pachic Xerumbrept
Musick	1390/1008–1688	Granodiorite (Dinkey Creek)	*Pinus ponderosa*; *Calocedrus decurrens*; *Quercus kelloggii*; *Chamaebatia foliolosa*	11.1	91	Fine-loamy, mixed, mesic; Ultic Haploxeralf
Auberry	794/595–1008	Tonalite (Blue Canyon)	*Quercus douglasii*; *Quercus wislizeni*; *Ceanothus* species; Annual grasses	14.4	62	Fine-loamy, mixed, thermic; Ultic Haploxeralf
Ahwahnee	561/258–595	Tonalite (Blue Canyon)	*Quercus douglasii*; *Quercus wislizeni*; *Pinus sabiniana*; *Ceanothus* species; Annual grasses	15.0	57	Coarse-loamy, mixed, thermic; Ultic Haploxeralf
Vista	198/ < 258	Tonalite (Blue Canyon)	Annual grasses; *Quercus douglasii*; *Quercus wislizeni*	16.7	33	Coarse-loamy, mixed, thermic; Typic Xerochrept

[a] Elevation for the site of soil sampling and the elevation range in which each series occurs along our transect.
[b] Data from Bateman and Lockwood (1970, 1976), and Bateman and Wones (1972).
[c] Vegetation listed in order of dominance.
[d] From regression equations of Harradine and Jenny (1958).
[e] Tentative soil series.
[f] Coarse fragments are < 5 mm in diameter.

Soil pH was measured in water and 0.01 *M* $CaCl_2$ (1:2, soil:water) following a 15-min equilibration period. Cation exchange capacity (CEC), exchangeable cations (Ca, Mg, K, Na), and base saturation were determined using 1 *M* NH_4OAc at pH = 7 (Soil Survey Staff, 1984). Total organic carbon and nitrogen were determined by dry combustion on samples ground to < 180 μm. Bulk density measurements were performed on field-moist, paraffin-coated peds when possible, or alternatively, by standard coring techniques (Soil Survey Staff, 1984).

Selective dissolution was performed as follows: (1) organically complexed Al and Fe by sodium pyrophosphate, one 16-h extraction (McKeague, 1967); (2) noncrystalline aluminosilicates and Fe-oxyhydroxides and organically complexed Fe and Al by acid ammonium oxalate, one 4-h extraction at pH 3 in the dark (McKeague, 1976); and (3) crystalline and noncrystalline Fe-oxyhydroxides and organically complexed Fe and Al by citrate-dithionite, one 16-h extraction at 23°C (Holmgren, 1967). Prior to centrifugation, 2 ml of 0.1% superfloc was added to each extract to assist in settling of dispersed colloidal material. Iron, Al and Si in all extracts were measured by inductively coupled plasma (ICP) spectrometry. All values represent the mean of duplicate analyses.

Particle-size distribution was determined by dry sieving and the pipette method (Soil Survey Staff, 1984) following organic matter removal with sodium hypochlorite (Lavkulich and Wiens, 1970), free iron oxide removal with citrate-dithionite (Holmgren, 1967), and dispersion with sodium hexametaphosphate. The clay-size fraction (< 2 μm) was isolated by flocculation with NaCl and sedimentation following particle-size analysis and desalted by dialysis against deionized water (18 MΩ). X-ray diffraction analysis was performed on oriented clays mounted on ceramic tiles following standard methods: Mg saturation, Mg saturation/glycerol solvation, Mg saturation/formamide solvation, K saturation, and heat treatment of the K-saturated tile at 350° and 550°C (Ross et al., 1983; Whittig and Allardice, 1986). Diffractograms were made on a Diano 8000 X-ray Diffractometer using Cu Kα radiation generated with 50 kV accelerating potential and 15 mA tube current. Samples were step scanned for 1 s at a 0.04 degree 2θ step. Based on peak intensity, the abundance of a given clay mineral was assigned a rating of major (3), moderate (2) or minor (1). The relative abundance within a given sample was calculated as the percentage of the total based on the numerical values assigned to each rating. Transmission electron microscopy (TEM) (Zeiss Model 109) was performed on the clay fraction and scanning electron microscopy (SEM) (Hitachi Model 450) was performed on the fine-sand fraction of the Musick soil (1390 m) to examine weathering and transformation products.

Solum (A and B horizons) concentrations of clay, citrate-dithionite extractable Fe, and organic carbon were calculated on a per area basis (kg/m^2). Calculations were based on horizon thickness and bulk density, and were corrected for the volume of coarse fragments (> 2-mm fraction).

To broaden the spatial scale and geographical significance of our study, data for solum depth, clay, organic carbon, and total nitrogen were obtained from three to seven additional pedons for each soil characterized as part of soil survey investigations in the central Sierra Nevada (Allardice et al., 1983; Soil Conservation Service, 1994) and from a pedological investigation of clay production along the lower half of the transect (Huntington, 1954). While the analytical methods may vary somewhat between studies,

these additional data representing typical pedons for each soil provide an important basis for comparison to the soils examined in this study. Differences in soil properties among soil series were examined using ANOVA with the soil property as the dependent variable and soil series as the independent variable. Pairwise comparisons between soil series were made using a post-hoc Fisher's LSD test at the $p = 0.05$ significance level.

3. Results and discussion

3.1. Soil morphology and classification

Maximum expression of many morphological properties are displayed at the mid-elevation range: solum depth, absence of coarse fragments (> 2-mm fraction), clay concentrations, argillic horizon development, and soil reddening (Table 2). Subsoil textural classes have the following distribution with increasing elevation: coarse sandy loams → sandy clay loams → loamy sands → loamy coarse sands. Clay translocation has occurred in the four soils at the lower elevations (< 1600 m) as indicated by increased clay content and the presence of clay films or lamellae in the B horizons. Clay lamellae are found in the lowest elevation soil (Vista 198 m) while clay concentrations and thickness of the argillic horizon increase with increasing elevation to a maximum in the Musick soil (1390 m). At approximately 1600 m there is an abrupt transition; soils above this elevation display no evidence of clay translocation and accumulation. Similarly, the B horizons become progressively redder with increasing elevation, reach a maximum redness in the Musick soil (1390 m), and abruptly change to less red hues and lower chromas in soils above 1600 m. All the soils along the transect are well drained and display no redoximorphic features. The soils above 1600 m have thicker and darker A horizons due to the accumulation of organic matter. At lower elevations organic horizons (Oi, Oe, and Oa) are often lacking under annual grass vegetation with up to 2 cm thickness under shrub and oak vegetation. They increase to a maximum of about 14 cm under mixed-conifer cover in the mid-elevations (Musick, 1390 m), then decrease with increasing elevation in the upper portion of the transect, becoming intermittent at the highest elevations in relation to a more open conifer cover. Associated with the thick organic horizons in the Musick are transitional AE and EBt horizons in which Fe appears to be eluviated by complexation with organic acids leaching from the O horizons.

Soil classification according to *Soil Taxonomy* is given in Table 1 (Soil Survey Staff, 1994). The soils above 1600 m have umbric or ochric epipedons (Sirretta just misses color requirement for umbric) and no diagnostic subsurface horizons leading to their classification as Umbrepts or Orthents. The umbric epipedon displays a maximum expression of 70 cm in the Shaver soil (1800 m) resulting in a pachic subgroup designation. Between 300 and 1600 m, the soils have ochric epipedons and argillic subsurface horizons and are classified as Haploxeralfs. Soils below 300 m are classified as Ochrepts with an ochric epipedon and a cambic subsurface horizon.

Table 2
Selected morphological properties for the seven typical pedons composing the elevational transect on granitic residuum on the western flank of the Sierra Nevada

Horizon	Depth (cm)	Boundary	Color		Texture	Structure	Consistence	Roots	> 2 mm (%)	Clay films
			dry	moist						
Chiquito (2865 m)										
Oi/Oa	3–0									
A1	0–6	cs	10YR 2/2	10YR 2/1	vgrlcos	1fgr	lo lo so po	1vf,1f	40	–
A2	6–15	gw	10YR 2/2	10YR 2/2	grlcos	1msbk	so vfr so po	2f,1m	32	–
A3	15–29	gw	10YR 3/3	10YR 3/2	vgrlcos	1msbk	so vfr so po	1f,2m	55	–
A4	29–42	gw	10YR 3/3	10YR 3/2	xklcos	1msbk	so vfr so po	1f,2m,3co	60	–
Bw	42–63	cw	10YR 5/4	10YR 4/3	vklcos	1fsbk	so vfr so po	2m	50	–
BC	63–81	ai	10YR 6/6	10YR 4/2	xklcos	sg	so vfr so po	–	60	–
R	81+									
Sirretta (2195 m)										
Oi	3–0									
A1	0–6	cs	2.5YR 4/2	10YR 2/1	gls	1vfgr	lo lo ss po	3vf	33[a]	–
A2	6–17	gs	10YR 5/3	10YR 3/3	glcos	1msbk	so vfr ss po	2vf	33	–
A3	17–29	gs	10YR 5/3	10YR 4/3	glcos	1msbk	so vfr ss po	2vf,1m,2co	25	–
Bw1	29–62	gs	2.5YR 6/4	10YR 5/4	vglcos	1msbk	so vfr ss po	2f,2m,2co	50	–
Bw2	62–89	aw	2.5YR 6/4	10YR 5/4	vglcos	1msbk	so vfr ss po	1f,1m,1co	50	–
Bw3	89–102	aw	2.5YR 7/2	10YR 5/4	vglcos	1msbk	so vfr ss po	1f,1m	55	–
CB	102–131	aw	2.5YR 6/4	10YR 5/4	glcos	sg	so vfr ss po	–	30	–
Cr	131+									
Shaver (1800 m)										
Oi	4–0									
A1	0–4	cs	10YR 5/3	10YR 2/2	ls	1fgr	lo lo so po	2vf,2f	< 10	–
A2	4–18	gs	10YR 5/3	10YR 2/2	ls	1fgr	so vfr so po	2f	< 10	–
A3	18–46	dw	10YR 5/3	10YR 3/3	ls	1msbk	sh fr so po	2f,2m	< 10	–
A4	46–70	dw	10YR 5/3	10YR 3/3	ls	1msbk	so vfr so po	2f,2m	< 10	–
Bw1	70–102	dw	10YR 6/3	10YR 3/4	ls	1csbk	so vfr so po	2f,2m,2co	< 10	–
Bw2	102–172	dw	10YR 6/2	10YR 5/2	ls	1csbk	so vfr so po	2f,2m	< 10	–
Cr	172+									

Musick (1390 m)										
Oi	14–8									
Oe/Oa	8–0									
AE	0–29	cw	10YR 6/3	10YR 5/4	sl	1msbk	sh fr ss ps	2vf,2f,2m,2co	< 10	–
EBt	29–38	aw	10YR 6/4	10YR 5/6	sl	1msbk	h fr ss ps	1vf,2f,2co	< 10	1mkpo
Bt1	38–54	cw	10YR 5/8	10YR 4/8	scl	2mpr	h fr ss ps	1f,2co	< 10	2kpo
Bt2	54–69	aw	2.5YR 5/6	2.5YR 4/6	scl	1mabk	h fr ss ps	1f,2m	< 10	2kpo
BCt1	69–96	cw	7.5YR 6/8	7.5YR 5/8	sl	1csbk	sh fr ss ps	1f,2m	< 10	2kpo
BCt2	96–180	cw	7.5YR 7/3	7.5YR 6/4	sl	1csbk	sh fr ss po	2m	< 10	2kpo
Cr	180+									
Auberry (794 m)										
Oi	2–0									
A1	0–5	cs	10YR 5/2	10YR 3/3	cosl	2f-mgr	sh fr so po	3f	< 10	–
A2	5–18	cs	10YR 6/3	10YR 4/2	cosl	1f-msbk	h fr so po	1f,1m	< 10	–
BAt	18–38	cs	10YR 5/3	10YR 4/3	sl	1msbk	h fr so po	1f,1m	< 10	1n po br
Bt1	38–70	as	10YR 5/3	10YR 4/4	scl	2cabk	vh fi ss ps	1f,1m	< 10	2mkpf
Bt2	70–115	gw	7.5YR 5/5	10YR 4/4	sl	1csbk	vh fi ss ps	1f,1m,1co	< 10	2npf
BC	115–140	cw	10YR 6/3	10YR 5/4	cosl	1f-msbk	sh fr ss po	–	10	–
Cr	140–152									
R	152+									
Ahwahnee (561 m)										
Oi	1–0									
A1	0–4	aw	10YR 5/2	10YR 3/2	cosl	2fgr	so fr ss po	2vf	< 10	–
A2	4–19	cs	10YR 5/2	10YR 3/2	cosl	m	sh fr ss po	1vf,1f	< 10	–
BA	19–40	gs	10YR 5/4	10YR 4/3	cosl	m	sh fr ss po	1vf,1f,1m,1co	< 10	1co
Bt	40–72	ai	10YR 5/4	10YR 4/3	cosl	m	h fr ss po	1f,1m,1co	< 10	2co,1br,1npo
Cr	72-98									
R	98+									

Table 2 (continued)

Horizon	Depth (cm)	Boundary	Color		Texture	Structure	Consistence	Roots	> 2 mm (%)	Clay films
			dry	moist						
Vista (198 m)										
A	0–14	aw	10YR 5/4	10YR 4/6	gcosl	2mgr	sh vfr so po	3vf	20	–
Bw1	14–19	aw	10YR 6/3	10YR 4/4	glcos	1msbk	sh vfr so po	2vf	15	–
Bw2	19–34	aw	10YR 5/3	10YR 4/6	glcos	1msbk	h vfr so po	1vf	33	–
Bt	34–56	aw	10YR 5/3	10YR 4/4	gcosl	m	h vfr so po	1vf	33	lamellae
Crt	56–71									
R	71+									

[a] Coarse fragments throughout this profile are < 5 mm in diameter.

Abbreviations:

Boundary: a = abrupt; c = clear; g = gradual; d = diffuse; s = smooth; w = wavy; i = irregular.

Texture: s = sand; l = loam; c = clay; co = coarse; g = gravel; k = cobble; v = very.

Structure: 1 = weak; 2 = moderate; sg = single grain; m = massive; vf = very fine; f = fine; m = medium; c = coarse; gr = granular; pr = prismatic; abk = angular blocky; sbk = subangular blocky.

Consistence: (Dry) lo = loose; so = soft; sh = slightly hard; h = hard; vh = very hard; (Moist) lo = loose; vfr = very friable; fr = friable; fi = firm; (Wet) so = nonsticky; ss = slightly sticky; po = nonplastic; ps = slightly plastic.

Roots: 1 = few; 2 = common; 3 = many; vf = very fine; f = fine; m = medium; co = coarse.

Clay films: 1 = few; 2 = common; n = thin; mk = moderately thick; k = thick; pf = ped faces; po = pores; br = bridges; co = colloid stains.

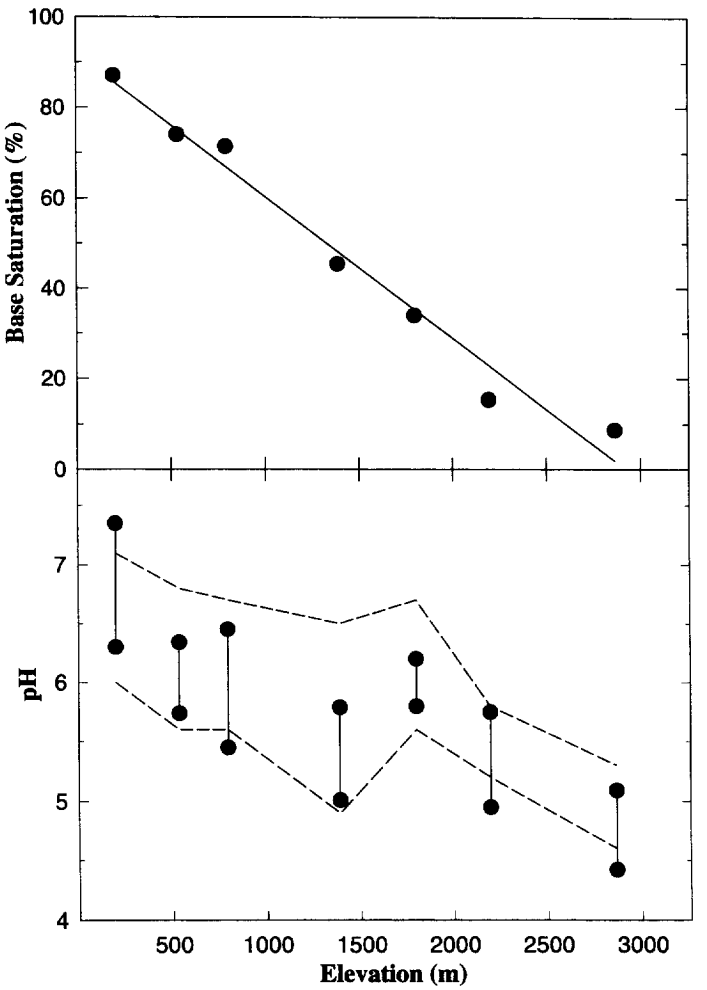

Fig. 2. Minimum and maximum pH values and base saturation along the elevational transect. In the pH graph, the vertical lines and dots indicate the pH range of the pedons sampled for this study and the dashed lines indicate the minimum and maximum soil pH values from soil survey characterization data ($n = 3$–5) in this area.

3.2. pH and base saturation

The minimum and maximum pH(H_2O) values show a decrease of approximately two units with increasing elevation and generally fall within the corresponding values obtained from soil survey characterization data (Fig. 2). A notable exception to the decrease in pH(H_2O) with increasing elevation was a pronounced increase (~ 0.75 units) from the Musick (1390 m) to the Shaver (1800 m) soils, which is also consistent with the soil survey characterization data. This suggests a threshold-type change in soil-forming processes occurring at about the 1600 m elevation.

Trends in pH(H_2O) and pH($CaCl_2$) within a profile were identical with the pH($CaCl_2$) values, an average of 0.75 units lower than corresponding pH(H_2O) values (Fig. 3). In some soils the highest pH values are found in the A horizons while in other profiles the highest values are found in the B horizons. The wide fluctuations in A horizon pH values along the transect (pH 4.4–6.5) probably result from differences in nutrient cycling characteristics by the contrasting vegetation. Except for the Shaver soil (1800 m), the B horizons of all soils above 1008 m had very similar pH values (5.0–5.2) (Fig. 3), possibly resulting from aluminum buffering in the pH range 4.5 to 5.0 (Ulrich, 1980).

Base saturation of the 0–18 cm depth shows a linear decrease with increasing elevation ($r^2 = 0.98$, $p < 0.001$) (Fig. 2). There is also a significant correlation ($r^2 = 0.70$, $p = 0.02$) between base saturation and pH(H_2O) reflecting the role of cation exchange reactions in buffering soil pH. The decrease in base saturation with elevation appears to be strongly linked to the leaching intensity, which increases with greater precipitation and lower evapotranspiration at the higher elevations (Jenny, 1941). Even at the lowest elevation, which receives 33 cm of precipitation, the leaching is sufficient to keep soluble salts and carbonates from accumulating in the solum.

3.3. CEC and exchangeable cations

Altitudinal trends in CEC were not strongly evident due to concomitant changes in organic matter concentration, clay content, and clay mineralogy along the transect. The CEC of A horizons ranged from 6 to 26.5 $cmol_c/kg$ and is related to organic C concentration (Table 3; Fig. 3). The CEC of the 0–18 cm layer generally increased with elevation (Table 3) and was strongly correlated with organic C concentration ($r^2 = 0.73$, $p = 0.014$). Within the B horizons, CEC values were similar (4–9 $cmol_c/kg$) for all soils in spite of a 7-fold difference in clay concentration, suggesting that soils with high clay concentrations are dominated by low CEC clays. Multiple linear regression analysis indicated a significant relationship between CEC and the independent variables organic carbon and clay concentrations ($r^2 = 0.87$, organic carbon $p < 0.001$; clay $p = 0.008$). This analysis predicted a CEC of 12 $cmol_c/kg$ clay and 238 $cmol_c/kg$ C, the latter being similar to the 240 $cmol_c/kg$ C determined by Parfitt et al. (1995). The value of 12 $cmol_c/kg$ clay is consistent with that of the low-activity clays found to dominate the clay mineralogy of these soils.

Exchangeable cation composition followed the trend Ca > K > Mg > Na for the three soils at high elevation (> 1600 m) and Ca > Mg > K > Na for the four soils at lower elevation (Table 3). The dominance of K compared to Mg in the upper elevation soils may reflect differences in the chemical composition of the parent material, nutrient cycling by contrasting vegetation, or cation selectivity due to variations in clay mineralogy.

3.4. Organic carbon and nitrogen

Soil organic matter concentrations depend on the complex interaction of several factors including the quantity and quality of litter fall, climatic factors, soil properties

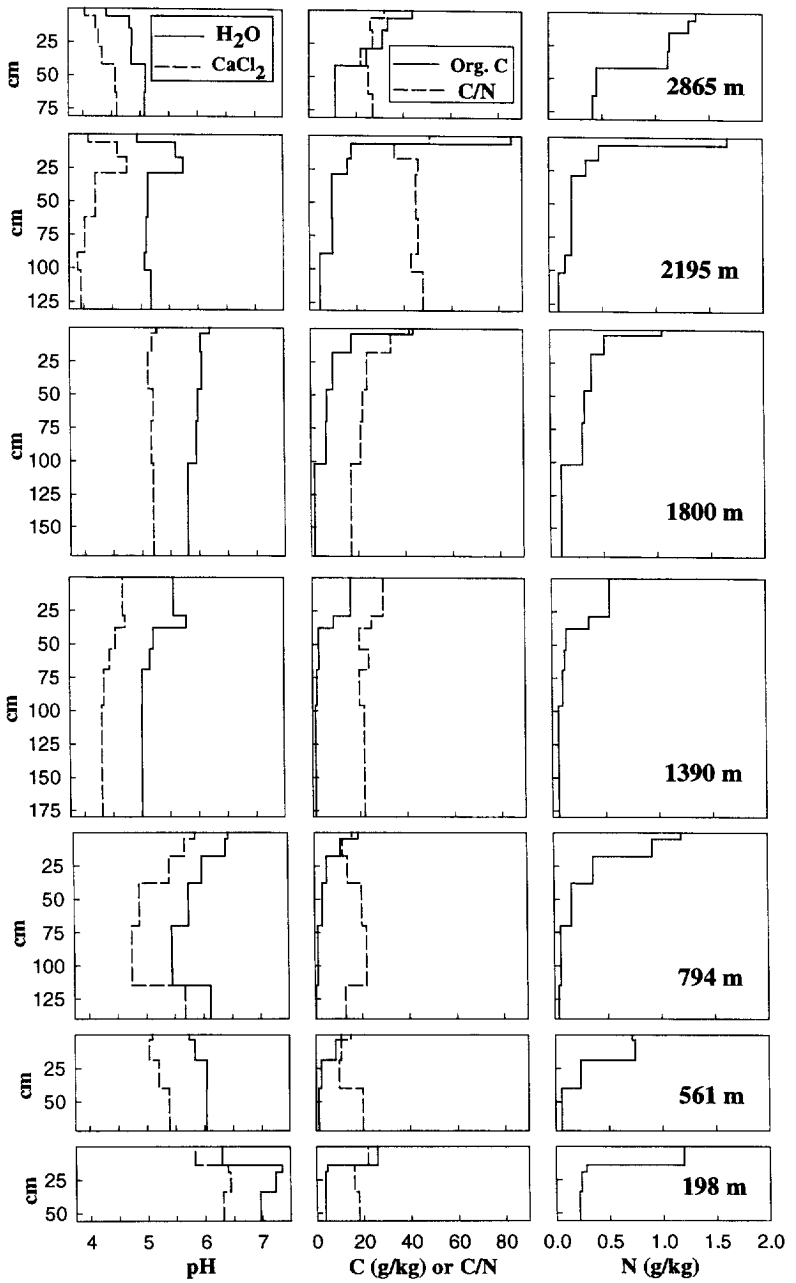

Fig. 3. Vertical distribution of pH, organic C, C/N ratio and N for the seven soils comprising the elevational transect.

(especially the amount and type of clay), and erosion. Jenny (1950) estimated that steady-state soil organic matter concentrations could be reached in 200 to 1000 years in the central Sierra Nevada; however, other data suggest that 10^4 years may be required to

Table 3
Cation exchange capacity, exchangeable cations, base saturation and particle size distribution for the seven pedons composing the elevational transect

Horizon	Depth	CEC	Exchangeable cations ($cmol_c$ /kg)				Base sat.	Sand	Silt	Clay
	(cm)		K	Na	Mg	Ca	(%)	(%)	(%)	(%)
Chiquito (2865 m)										
A1	0–6	14.4	0.16	0.01	0.05	1.18	10	80	16	4
A2	6–15	12.2	0.16	0.02	< 0.01	0.89	9	81	15	4
A3	15–29	10.5	0.12	0.02	< 0.01	0.55	7	81	15	4
A4	29–42	9.5	0.08	0.02	< 0.01	0.39	5	81	15	4
Bw	42–63	6.2	0.06	0.01	< 0.01	0.12	3	84	13	3
BC	63–81	6.3	0.06	0.01	< 0.01	0.15	4	83	13	4
Sirretta (2195 m)										
A1	0–6	26.5	0.31	0.02	0.21	3.36	15	80	15	5
A2	6–17	11.5	0.28	0.02	0.09	1.43	16	78	16	6
A3	17–29	9.1	0.34	0.01	0.13	1.04	17	77	16	7
Bw1	29–62	7.7	0.18	0.02	0.10	0.23	7	95	2	3
Bw2	62–89	8.5	0.15	0.02	0.13	0.16	5	87	9	4
Bw3	89–102	9.2	0.13	0.03	0.10	0.12	4	79	16	5
CB	102–131	7.8	0.08	0.03	0.05	0.06	3	81	13	6
Cr	131+	4.2	0.05	0.01	< 0.01	0.03	2	78	15	7
Shaver (1800 m)										
A1	0–4	18.0	0.36	0.01	0.29	7.67	46	80	15	5
A2	4–18	10.9	0.27	0.01	0.16	2.88	31	79	17	4
A3	18–46	9.9	0.27	0.01	0.14	1.77	22	83	13	6
A4	46–70	9.2	0.40	0.02	0.21	2.50	34	80	15	8
Bw1	70–102	8.7	0.50	0.01	0.14	2.96	41	80	15	8
Bw2	102–172	5.1	0.15	0.01	0.55	3.32	79	83	13	6
Cr	172+	5.7	0.09	0.03	0.58	3.18	68	85	12	3
Musick (1390 m)										
AE	0–29	11.9	0.48	0.04	1.34	3.53	45	60	27	15
EBt	29–38	9.2	0.43	0.04	1.24	3.29	54	62	24	16
Bt1	38–54	8.6	0.34	0.03	1.29	2.64	50	64	14	27
Bt2	54–69	8.4	0.26	0.03	1.17	2.35	46	63	16	25
BCt1	69–96	8.8	0.23	0.05	1.16	2.09	40	67	18	17
BCt2	96–180	8.0	0.17	0.04	1.29	1.67	39	76	17	11
Auberry (794 m)										
A1	0–5	10.5	0.34	0.02	0.91	5.95	69	72	19	9
A2	5–18	8.3	0.32	0.02	0.76	5.03	74	70	21	9
BAt	18–38	7.4	0.21	0.03	0.73	4.54	75	64	25	11
Bt1	38–70	7.1	0.16	0.10	1.60	4.21	86	56	24	20
Bt2	70–115	6.7	0.07	0.09	1.65	3.56	80	64	23	13
BC	115–140	5.3	0.05	0.07	1.52	3.02	88	74	19	7

Table 3 (continued)

Horizon	Depth (cm)	CEC	Exchangeable cations ($cmol_c$ /kg)				Base sat. (%)	Sand (%)	Silt (%)	Clay (%)
			K	Na	Mg	Ca				
Ahwahnee (561 m)										
A1	0–4	7.5	0.21	0.03	0.32	4.47	67	73	21	9
A2	4–19	6.1	0.18	0.02	0.34	3.98	74	72	22	12
BA	19–40	5.6	0.15	0.03	0.28	3.45	85	74	19	14
Bt	40–72	5.5	0.12	0.02	0.27	2.56	72	76	16	16
Cr	72–98	3.3	0.18	0.02	0.21	2.01	73	78	18	4
Vista (198 m)										
A	0–14	11.5	0.61	0.02	1.07	8.57	89	79	11	10
Bw1	14–19	6.5	0.20	0.03	0.65	4.31	80	80	12	8
Bw2	19–34	7.0	0.13	0.05	0.78	4.49	78	79	13	8
Bt	34–56	7.1	0.09	0.08	0.83	4.81	82	76	14	10

attain steady-state (Schlesinger, 1991). In this study, all soils appeared undisturbed and the climate since deglaciation has presumably varied little (Anderson, 1990; Scuderi, 1993); thus, we assume that soil organic matter concentrations were at or near steady-state with respect to the current soil-forming environment.

Formation of organic horizons (Oi, Oe, Oa) at the surface of the mineral soil reaches a maximum in the mid-elevation Musick soil (1390 m) and decreases at both higher and lower elevations (Table 2). The organic horizon thickness parallels closely the standing biomass and annual litter fall inputs (Jenny et al., 1949). Jenny et al. (1949) showed that these mid-elevation soils have the highest litter decomposition rates, indicating that litter fall production is a very important factor contributing to the thick organic horizons.

Solum organic C concentrations generally increase with increasing elevation ($r^2 = 0.40$; $p < 0.001$) (Fig. 4). Solum organic C concentrations within a given soil series vary spatially with coefficients of variation from 18 to 42%. This magnitude of variability is consistent with other studies of spatial variation in soil nutrient pools (Beckett and Webster, 1971; Grieve et al., 1990). Statistical analysis ($p < 0.05$) separates solum organic C pools into two groups consisting of lower concentrations (4.8–5.7 kg/m^2) below 1008 m and higher concentrations (10.5–14.7 kg/m^2) above 1008 m (Table 4). This separation occurs at the boundary between oak woodland and mixed-conifer-dominated forests. There is also an indication that solum organic C concentrations decrease in the highest-elevation soil (Chiquito 2865 m) consistent with lower standing biomass and litter fall production in these subalpine forests (Jenny et al., 1949).

Concentrations of organic C in the 0–18 cm depth (epipedon) show a similar trend ($r^2 = 0.45$; $p < 0.001$) to that of solum C concentrations (Table 4; Fig. 5). Organic C ranges from 10.1 g/kg in the Auberry soil (794 m) to a maximum of 32.4 g/kg in the Sirretta soil (2195 m) with an approximate 3-fold increase in organic C concentrations occurring between the Auberry (794 m) and Musick (1390 m) soils. High spatial variability is indicated by coefficients of variation ranging between 22 and 56%. The large increase in organic C between the Auberry and Musick soils corresponds to the elevation zone where mixed-conifer species replace oak woodlands as the dominant

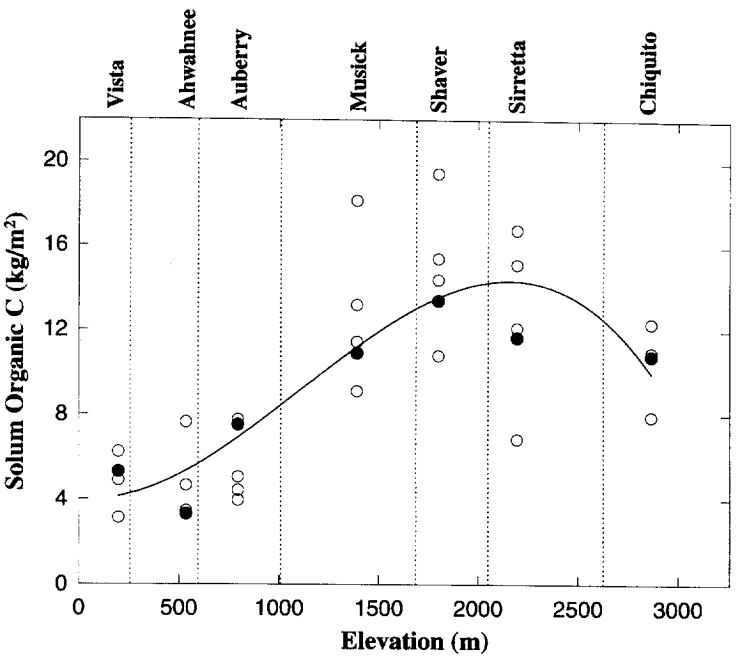

Fig. 4. Solum (A and B horizons) concentrations of organic carbon for the seven soils composing the elevational transect. Dots represent data analyzed in this study and circles represent data from soil survey characterization data ($n = 3$–5) in this area. The line represents the mean of all data points for each soil.

vegetation. A notable exception to the trend of increasing organic C with elevation is the decrease observed between the Vista (198 m) (17.8 g/kg) and the Ahwahnee (561 m) and Auberry (794 m) soils (10–12 g/kg). The oak woodland at the lowest elevation (Vista 198 m) has a dense annual grass understory that incorporates organic matter into the A horizon through root turnover. In contrast, the oak woodlands at 300–1000 m have a shrub-dominated understory that primarily contributes litter to the soil surface.

There was no significant ($p < 0.05$) trend in N concentrations in the 0–18 cm depth with elevation (Fig. 5). Nitrogen concentrations ranged from 0.4 to 1.8 g/kg with high spatial variability (coefficients of variation of 23 to 45%). In contrast, Harradine and Jenny (1958) found an increase in N concentrations with increasing elevation on the western slopes of the Sierra Nevada. Our results also differ from other studies that show both organic C and nitrogen content increasing exponentially with increasing altitude (summarized by Jenny, 1941). Similar to N concentrations in the 0–18 cm depth, concentrations of N in the solum showed no significant ($p < 0.05$) differences along the transect, ranging from 0.27 to 0.54 kg/m^2 in the seven soils analyzed for this study. There was insufficient data available from the soil survey investigations to determine solum N pools for the larger data set.

The C/N ratio of organic matter in the 0–18 cm depth generally increased with increasing elevation ($r^2 = 0.59$; $p < 0.001$) (Fig. 5). Further statistical analysis indicates lower C/N ratios (12–18) in the lowest three soils (< 1008 m) and higher values

Table 4
Statistical comparison of C and N concentrations and C/N ratio in the 0–18 cm fraction, solum concentrations of organic carbon and clay, and solum depth for seven soils representing an elevational transect in the western Sierra Nevada

	0–18 cm depth			Solum		
	Organic C (g/kg)	Total N (g/kg)	C/N	Organic C (kg/m^2)	Clay (kg/m^2)	Depth (cm)
Chiquito	30.4 b [a]	0.98 a	32.0 b	10.5 ab	31.5 a	70.5 a
2626–3259 m	$n = 4$	$n = 4$	$n = 4$	$n = 4$	$n = 4$	$n = 4$
Sirretta	32.4 b	1.04 a	32.0 b	12.5 b	57.8 a	104.2 b
2050–2626 m	$n = 5$	$n = 5$	$n = 5$	$n = 5$	$n = 5$	$n = 5$
Shaver	29.4 b$n = 5$	1.15 a	27.4 b	14.7 b	175.3 c	173.3 c
1688–2050 m		$n = 5$	$n = 5$	$n = 5$	$n = 7$	$n = 5$
Musick	27.4 b	1.02 a	27.8 b	12.6 b	535.8 e	176.8 c
1008–1688 m	$n = 5$	$n = 5$	$n = 5$	$n = 5$	$n = 7$	$n = 5$
Auberry	10.1 a	0.81 a	12.4 a	5.7 a	301.8 d	119.0 b
595–1008 m	$n = 5$	$n = 5$	$n = 5$	$n = 5$	$n = 5$	$n = 5$
Ahwahnee	11.8 a	0.86 a	13.1 a	4.8 a	167.1 bc	78.5 a
258–595 m	$n = 4$	$n = 4$	$n = 4$	$n = 4$	$n = 4$	$n = 4$
Vista	17.8 ab	0.98 a	17.8 a	4.9 a	79.4 ab	57.0 a
164–258 m	$n = 4$	$n = 4$	$n = 4$	$n = 4$	$n = 7$	$n = 4$

[a] Values in each column followed by the same letter are not significantly different ($p < 0.05$).

(27–32) in the upper elevation soils (Table 4). This pattern in C/N ratios reflects the greater concentrations of organic C at higher elevations as N concentrations remained relatively constant along the transect. The large shift in C/N ratios occurs at the elevation where oak-woodland-dominated ecosystems are replaced by mixed conifers (Table 1), a pattern similar to that shown by Alexander et al. (1993) in northern California. Thus, litter quality may play an important role in regulating the C/N ratios. Lower C/N ratios may also result from a greater degree of decomposition at the low-elevation sites due to shorter organic C turnover times (litter inputs/decomposition rate) (Trumbore et al., 1996). Thus, the low-elevation sites have less fresh litter material and a shorter mean residence time contributing to a lower C/N ratio.

Soil organic C concentrations along the elevational transect correspond very closely with those of comparable ecosystem types. The oak woodlands and mixed-conifer forests in this study contained 4.8–5.7 and 10.5–14.7 kg C/m^2, respectively, compared to mean values of 6.9 and 11.8 kg C/m^2 for woodland and temperate forest ecosystems, respectively (Schlesinger, 1991). Organic C concentrations along this transect are somewhat lower than those of oak woodlands (9 kg C/m^2) and mixed-conifer forests (11–25 kg C/m^2) on volcanic soils in the Cascade Range of northern California (Alexander et al., 1993). Increasing organic C concentrations with increasing elevation is

a common feature of attitudinal transects of soils throughout the world (e.g., Hanawalt and Whittaker, 1976; Amundson et al., 1989; Grieve et al., 1990; Tate, 1992; Alexander et al., 1993). The trend of decreased organic C at the highest elevation site of this

Table 5
Selective dissolution data characterizing various crystalline and non-crystalline forms of iron, aluminum and silicon

Horizon	Depth (cm)	Si_o [a] (g/kg)	Fe_o (g/kg)	Al_o (g/kg)	Fe_d [a] (g/kg)	Fe_p [a] (g/kg)	Al_p (g/kg)	$Al_o - Al_p$ (g/kg)	Fe_d / Fe_o
Chiquito (2865 m)									
A1	0–6	0.3	2.0	3.2	2.3	0.8	2.6	0.6	1.2
A2	6–15	0.3	2.0	3.5	2.7	0.9	2.8	0.7	1.4
A3	15–29	0.5	1.8	3.8	2.9	0.9	2.7	1.1	1.6
A4	29–42	0.7	2.1	4.4	2.9	0.6	2.6	1.8	1.4
Bw	42–63	1.2	1.8	4.9	2.3	0.5	1.8	3.1	1.3
BC	63–81	1.2	1.4	5.0	2.2	0.5	1.7	3.3	1.6
Sirretta (2195 m)									
A1	0–6	0.1	3.9	3.2	4.6	0.8	2.7	0.5	1.2
A2	6–17	0.3	3.9	3.7	4.9	0.5	2.2	1.5	1.3
A3	17–29	0.6	4.2	3.6	5.0	0.4	1.5	2.1	1.2
Bw1	29–62	0.3	3.3	2.4	4.1	0.4	1.3	1.1	1.2
Bw2	62–89	0.3	2.7	2.3	4.4	0.4	1.1	1.2	1.6
Bw3	89–102	0.3	1.5	2.1	7.5	0.2	0.9	1.2	5.0
CB	102–131	0.4	1.2	2.0	5.4	0.1	0.7	1.3	4.6
Cr	131+	0.4	0.9	1.6	2.2	< 0.1	0.4	1.2	2.4
Shaver (1800 m)									
A1	0–4	1.0	2.7	6.1	4.2	0.8	2.7	3.4	1.6
A2	4–18	1.1	2.8	6.6	4.4	0.6	2.7	3.9	1.6
A3	18–46	0.9	2.6	4.4	4.3	0.8	1.9	2.5	1.6
A4	46–70	1.2	2.6	5.3	4.6	0.7	1.5	3.8	1.8
Bw1	70–102	0.9	2.6	3.9	4.3	0.6	1.3	2.6	1.6
Bw2	102–172	0.2	1.8	0.5	3.6	0.2	0.1	0.4	2.0
Cr	172+	0.2	1.4	0.4	3.7	0.1	0.1	0.3	2.6
Musick (1390 m)									
AE	0–29	0.1	1.0	1.1	7.6	0.9	1.1	< 0.1	7.7
EBt	29–38	0.1	0.8	0.9	9.3	0.8	0.7	0.2	11.1
Bt1	38–54	0.1	0.8	0.9	14.4	0.1	0.3	0.6	16.7
Bt2	54–69	0.1	0.8	0.8	11.9	0.1	0.3	0.5	14.3
BCt1	69–96	0.1	0.9	0.8	10.3	0.1	0.2	0.6	11.1
BCt2	96–180	0.1	0.6	0.6	7.0	0.1	0.2	0.4	11.1
Auberry (794 m)									
A1	0–5	0.1	0.8	0.9	6.5	0.4	0.6	0.3	8.3
A2	5–18	0.1	0.7	0.8	8.4	0.2	0.3	0.5	12.5
BAt	18–38	0.1	0.6	0.7	8.5	0.1	0.2	0.5	14.3
Bt1	38–70	0.1	0.6	0.7	5.2	0.1	0.2	0.5	8.3
Bt2	70–115	0.1	0.5	0.7	4.2	0.1	0.1	8.3	0.6
BC	115–140	0.1	0.6	0.6	3.9	0.1	0.1	6.7	0.5

Table 5 (continued)

Horizon	Depth (cm)	Si_o [a] (g/kg)	Fe_o (g/kg)	Al_o (g/kg)	Fe_d [a] (g/kg)	Fe_p [a] (g/kg)	Al_p (g/kg)	$Al_o - Al_p$ (g/kg)	Fe_d / Fe_o
Ahwahnee (561 m)									
A1	0–4	0.1	0.7	0.7	5.6	0.3	0.2	0.5	7.7
A2	4–19	0.1	0.7	0.7	6.4	0.2	0.1	0.6	7.7
BA	19–40	0.1	0.6	0.6	5.9	0.1	0.1	0.5	8.3
Bt	40–72	0.1	0.5	0.5	5.2	0.1	0.1	0.4	8.3
Cr	72–98	0.1	0.6	0.4	3.9	0.1	0.1	0.3	6.7
Vista (198 m)									
A	0–14	0.1	0.6	0.3	4.3	0.2	0.2	0.1	7.1
Bw1	14–19	0.1	0.7	0.4	4.6	0.1	0.1	0.3	11.1
Bw2	19–34	0.1	0.7	0.4	5.3	0.1	0.1	0.3	7.7
Bt	34–56	0.1	0.6	0.4	5.2	< 0.1	0.1	0.1	8.3

[a] Abbreviations: o = acid oxalate, d = citrate-dithionite, p = pyrophosphate.

transect is not commonly observed and appears to result from reduced litter fall production due to lower standing biomass, and possibly by erosion of hydrophobic litter during summer convective storms.

The quantity and quality of litter fall and the decomposition rates are the important factors regulating forest floor and solum organic carbon concentrations along this transect. The highest organic matter concentrations occur in the mid-elevations of the transect where litter fall and decomposition rates are the greatest (Jenny et al., 1949). At low elevations, decomposition occurs mainly during the late-fall to spring rainy season. The high summer temperatures are ineffective for decomposition because of the severe moisture deficit. Decomposition at high elevations is limited to a very short period of time in the early fall and late spring. Microbial activity is limited by cold soil temperatures during the winter and a moisture deficit in the summer when soil temperatures are warmer. Litter quality may also contribute to the pattern of organic carbon and nitrogen accumulation along the transect.

3.5. Selective dissolution analysis

Organically complexed Al, extracted by pyrophosphate (Al_p), was very low (< 1 g/kg) in the four lower-elevation soils (< 1600 m) and increased to 1–2.8 g/kg in the high-elevation soils (Table 5). At higher elevations, larger concentrations of organic matter combined with lower pH values enhance formation of metal-humus complexes. However, the organic carbon concentrations are only weakly correlated with Al_p ($r^2 = 0.52$, $p < 0.001$) and Fe_p ($r^2 = 0.44$, $p < 0.001$). In contrast to Al, organically complexed Fe (Fe_p) was always < 1 g/kg. Since Fe is more stable in Fe oxyhydroxides than in humic complexes, it is common for organically complexed Fe to be very low (Wada and Higashi, 1976).

Acid oxalate extractable Si (Si_o) originates primarily from noncrystalline aluminosilicates, such as allophane and imogolite (Childs et al., 1983). The low Si_o levels (< 1.2

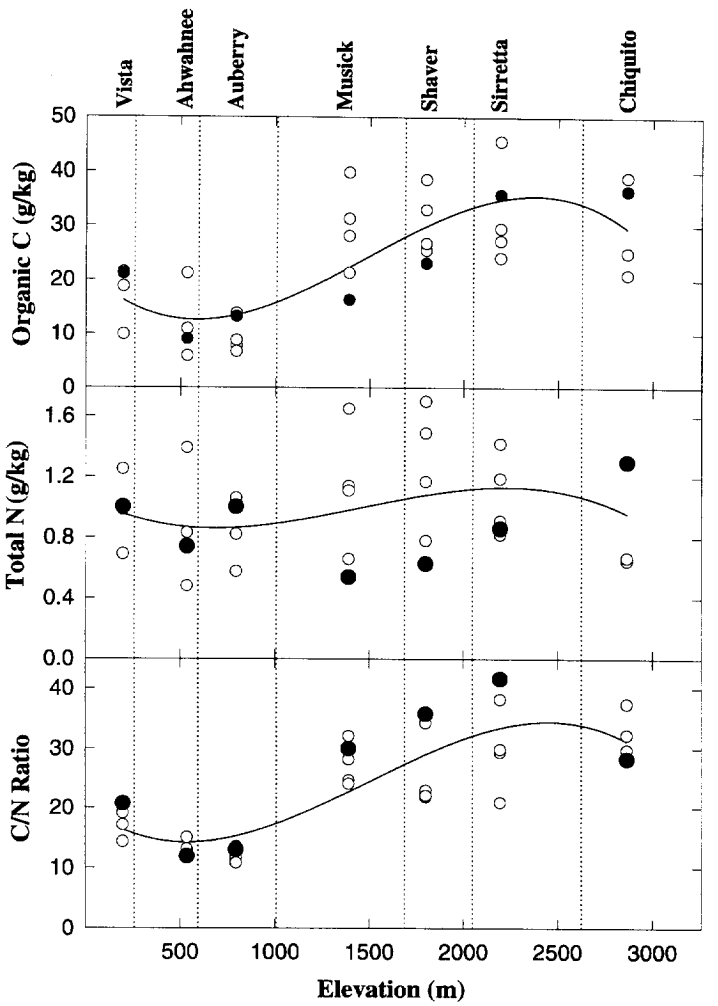

Fig. 5. Organic carbon, nitrogen and C/N ratio in the 0–18 cm depth for the seven soils composing the elevational transect. Dots represent data analyzed in this study and circles represent data from soil survey characterization data ($n = 3$–5) in this area. The line represents the mean of all data points for each soil.

g/kg) observed throughout the transect indicate that no appreciable concentration of noncrystalline aluminosilicates was present (Table 5). Noncrystalline inorganic forms of Al were estimated by the difference between oxalate extractable Al (Al_o) and Al_p. The Al_o–Al_p concentrations were generally low (< 4 g/kg) with larger values observed in the high-elevation soils (> 1600 m) (Table 5). Since noncrystalline aluminosilicates were not detected, the Al_o–Al_p quantity probably represents the partial extraction of the hydroxy-Al interlayer from 2 : 1 layer silicates and gibbsite (Iyengar et al., 1981; Parfitt and Childs, 1988), which are the dominant clay minerals in the upper elevation soils. The low levels of Al_o indicate that most of the Al released from primary mineral

weathering is incorporated into crystalline clay minerals. In the absence of Fe-humus complexes, acid oxalate extractable Fe (Fe_o) originates primarily from the dissolution of the noncrystalline Fe oxyhydroxide, ferrihydrite (Schwertmann, 1985). Relatively high concentrations of Fe_o (1.4–3.1 g/kg) were found in the upper elevation soils (> 1600 m) compared to concentrations < 1 g/kg below 1600 m elevation.

Dithionite-citrate extractable Fe (Fe_d) is a useful indicator of the amount of Fe released by weathering in well-drained soils that are not strongly acid. The highest Fe_d concentrations were found in the mid-elevations and concentrations dropped notably at both higher and lower elevations (Table 5). The highest Fe_d concentrations generally correspond to the reddest hue and highest chroma along the transect (Table 2). The ratio, Fe_d/Fe_o, provides an estimate of the degree of crystallinity for Fe oxides. The Fe_d/Fe_o ratios were high (> 6) in the low-elevation soils (< 1600 m) and decreased (< 3) in the high-elevation soils. The high ratios at low elevations indicate a high degree of Fe-oxide crystallinity in these soils compared to the upper elevation soils. Cold soil temperatures and the higher concentrations of organic matter both interfere with the crystallization process and likely contribute to this pattern (Schwertmann, 1985).

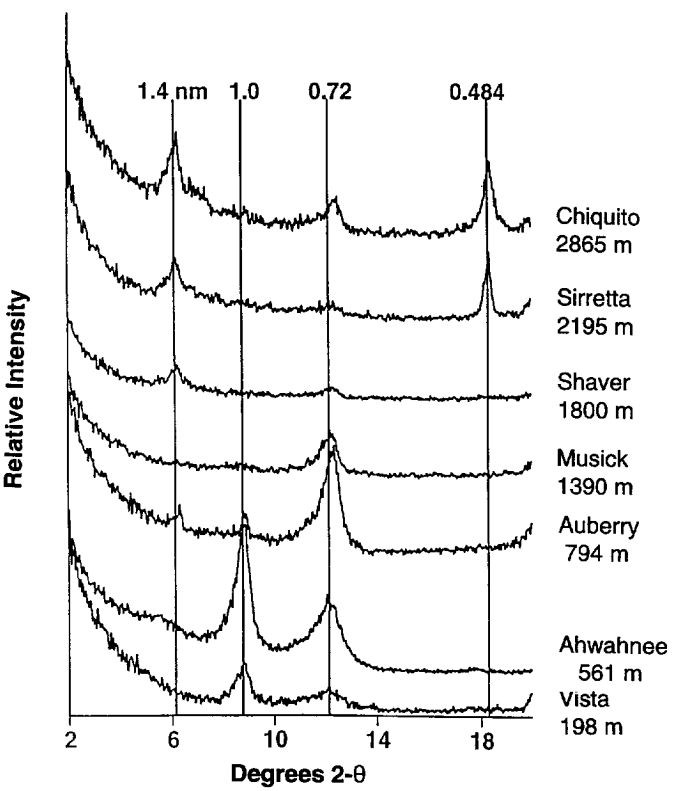

Fig. 6. XRD diffractograms of Mg-saturated clay specimens from the 50-cm depth for the seven soils composing the elevational transect.

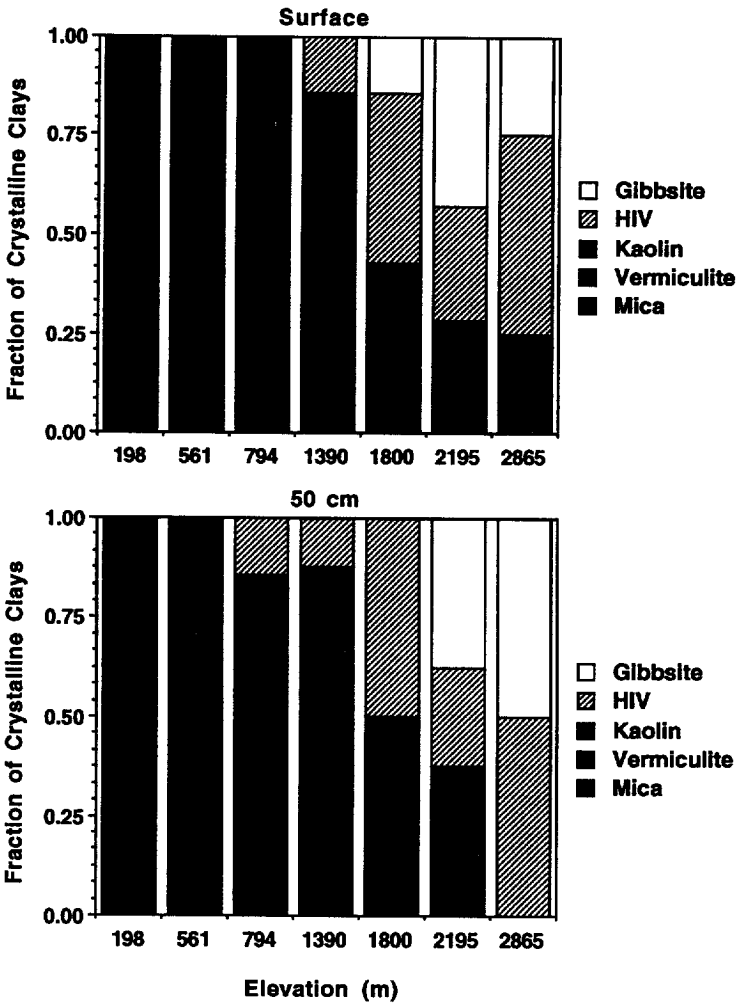

Fig. 7. Relative abundance of clay minerals in the clay-size fraction from the surface and 50-cm depths for the seven soils composing the elevational transect.

3.6. Clay mineralogy

The distribution of clay minerals indicated by XRD analysis is relatively uniform with depth within a given soil profile. The clay mineralogy displays a general trend of desilication and hydroxy-Al interlayering of 2 : 1 layer silicates with increasing elevation (Figs. 6 and 7). This pattern is consistent with the increase in leaching potential that occurs with increasing elevation.

3.6.1. Low-elevation zone (100–1008 m elevation)

Soils in the low-elevation zone display low to moderate intensity weathering limited by the lack of soil moisture for the majority of the year. Plagioclase, K-feldspar, biotite,

and muscovite are most susceptible to weathering and therefore have a major influence on clay mineralogy in soils derived from granitic parent material. Under the low-intensity leaching regime, primary mica is altered predominantly to an illite phase by partial removal of K from the interlayer as evident in all three low-elevation soils. With a slightly greater leaching intensity, mica decreases and a minor component of vermiculite occurs in the Ahwahnee (561 m) and Auberry (794 m) soils. Traces of hydroxy-Al interlayered vermiculite appear in the subsoil of the Auberry (794 m) soil as the soil pH is lowered into the range 5–6. Plagioclase alters to kaolinite in the Vista (198 m) and Ahwahnee (561 m) soils and to a mixture of kaolinite and halloysite in the Auberry (794 m) soil. Halloysite is probably the initial weathering product of plagioclase, subsequently dehydrating to exhibit XRD characteristics similar to kaolinite, a transformation occurring in other soils in the xeric moisture regime of California (Southard and Southard, 1987; Takahashi et al., 1993).

3.6.2. Mid-elevation zone (1008–1600 m)

The mid-elevation zone has moderate temperature and precipitation and displays the greatest weathering intensity along the transect. The clay mineralogy typified by the Musick soil (1390 m) is dominated by kaolin minerals. Kaolinite is dominant in the surface horizons and halloysite is dominant in the deepest horizon. Scanning electron microscopy of sand grains showed pseudomorphic replacement of plagioclase by tubular halloysite as previously shown by Southard and Southard (1987). Halloysite is susceptible to dehydration during the prolonged summer moisture deficit, especially at the soil surface. Transmission electron microcopy showed an abundance of tubular and few plate-like crystals in the clay fractions throughout the Musick (1390 m) profile. Thus, we conclude that the halloysite to kaolinite transformation involves a dehydration step with no appreciable change in morphology.

Mica is still evident in the clay fraction throughout the Musick (1390 m) profile, but is much less abundant than in soils at lower elevations. The mica appears to weather to vermiculite that rapidly becomes hydroxy-Al interlayered under favorable pH conditions ($pH(H_2O) = 5.0–5.8$) (Barnhisel and Bertsch, 1989). Given the dominance of kaolin minerals, it is also possible that mica has been desilicated to form a 1 : 1 layer silicate (Yatsu, 1988).

3.6.3. High-elevation zone (1600–2900 m)

The high-elevation weathering environment is characterized by cool to cold soil temperatures and intense leaching resulting from the spring melting of the winter snowpack. The clay mineralogy is dominated by hydroxy-Al interlayered vermiculite and gibbsite. The kaolin minerals decreased with increasing elevation, possibly being weathered to gibbsite. Gibbsite may also precipitate from Al released during the weathering of feldspar and plagioclase under intense leaching environments (Hsu, 1989). Hydroxy-Al interlayering of vermiculite enhances the stability of 2 : 1 layer silicates (Karathanasis, 1988) which probably explains its abundance in these high-elevation soils. Only traces of mica and vermiculite were observed by XRD. The dominance of Al-rich/Si-depleted minerals suggests that the weathering environment is very effective at removing Si released by weathering in spite of the cold soil temperatures. Thus, it

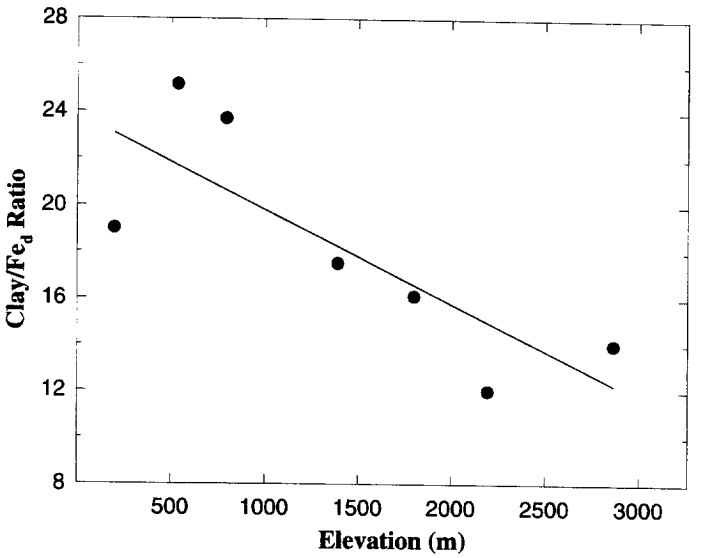

Fig. 8. The clay/secondary iron oxide ratio for the seven soils composing the elevational transect. Ratios are based on solum (A and B horizons) concentrations computed on a kg/m^2 basis. The line is the regression for all data points.

appears that leaching intensity rather than soil temperature determines the degree of desilication and pathways of mineralogical transformation along this transect.

3.6.4. Effect of climate on clay mineralogy and the degree of weathering

The desilication pattern with increasing precipitation is further supported by the ratio of clay to secondary Fe (Fe_d) calculated on a solum basis (kg/m^2). Since Fe is relatively immobile in well-drained soils at the pH conditions existing along the transect, Fe_d is used in this ratio as a conservative element and an indicator of weathering. The clay/Fe_d ratio of the sampled pedons shows a general decrease from 26 to 13 with increasing elevation ($r^2 = 0.71$, $p = 0.02$) (Fig. 8). Some of the scatter that exists for this ratio may result from differences in lithologies of the parent material (e.g., granodiorite versus tonalite; Table 1). The two-fold difference in this ratio suggests that twice as much clay is produced per unit of weathering in the low-elevation soils as compared to the high-elevation soils. As the leaching intensity increases with increasing elevation, there is a greater loss of weathering products (primarily Si) resulting in less reactants to form aluminosilicate clay minerals.

The generalized weathering pathway of progressive desilication is consistent with other studies of clay mineralogy on granitic parent materials (reviewed by Yatsu, 1988) (Fig. 9). Similar results were also obtained for clay mineralogical studies on granitic parent materials in California (Barshad, 1966; Nettleton et al., 1968), except we did not find smectite in the warmer, drier climatic regime at low elevation. Barshad (1966) also reported that kaolin minerals were the dominant clay constituent at precipitation amounts > 50 cm, but he limited his investigation to soils with mean annual air

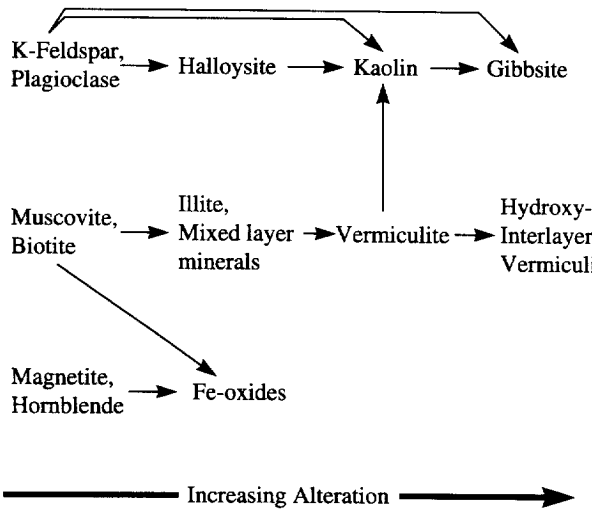

Fig. 9. A generalized weathering pathway for granitic parent materials of this study as a function of increasing weathering intensity.

temperatures between 10° and 16°C, comparable to the 300–1600 m zone of our study. We found that hydroxy-Al interlayered vermiculite and gibbsite dominate above 1600 m. Barshad (1966) did not specifically report the presence of hydroxy-Al interlayered vermiculite, but it may be included in his vermiculite category.

Three parameters were used to quantify the amount of weathering along the transect. These measures included solum depth and the concentrations of clay and Fe_d in the solum. The depth of the solum is a measure of the balance between erosion and the combined effects of both physical and chemical weathering processes. Solum depth was greatest at the mid-elevations (1008–2050 m) and decreased significantly ($p < 0.05$) at both lower and higher elevations (Table 4; Fig. 10). In the mid-elevation zone associated with the Musick soil (1390 m), decomposed rock may extend to a depth of 30 m as shown in road cuts (Allardice et al., 1983). There is a virtual absence (< 10%) of coarse fragments (> 2 mm) in soils between 300 and 2050 m (Table 2). In contrast, soils at the drier (low elevation) and colder (upper elevation) ends of the transect have appreciable concentrations (up to 60% by volume) of coarse fragments within the solum. While solum depths are similar between the Musick (1390 m) and Shaver (1800 m) soils (177 and 173 cm), indicators of chemical weathering (solum clay and Fe_d concentrations) are much greater for Musick than for Shaver soils (Fig. 10).

Physical weathering of granitic bedrock to grus results, in large part, from hydration of biotite (Wahrhaftig, 1965; Nettleton et al., 1968). Biotite swells by approximately 30% upon partial alteration and hydration creating many microfractures between the larger grains that lead to shattering of the rock fabric. The occurrence of continuously moist conditions greatly enhances this grus-forming process (Wahrhaftig, 1965). The low-elevation soils are extremely dry for approximately six months (May–October) of the year which would reduce physical weathering. In contrast, the high-elevation soils

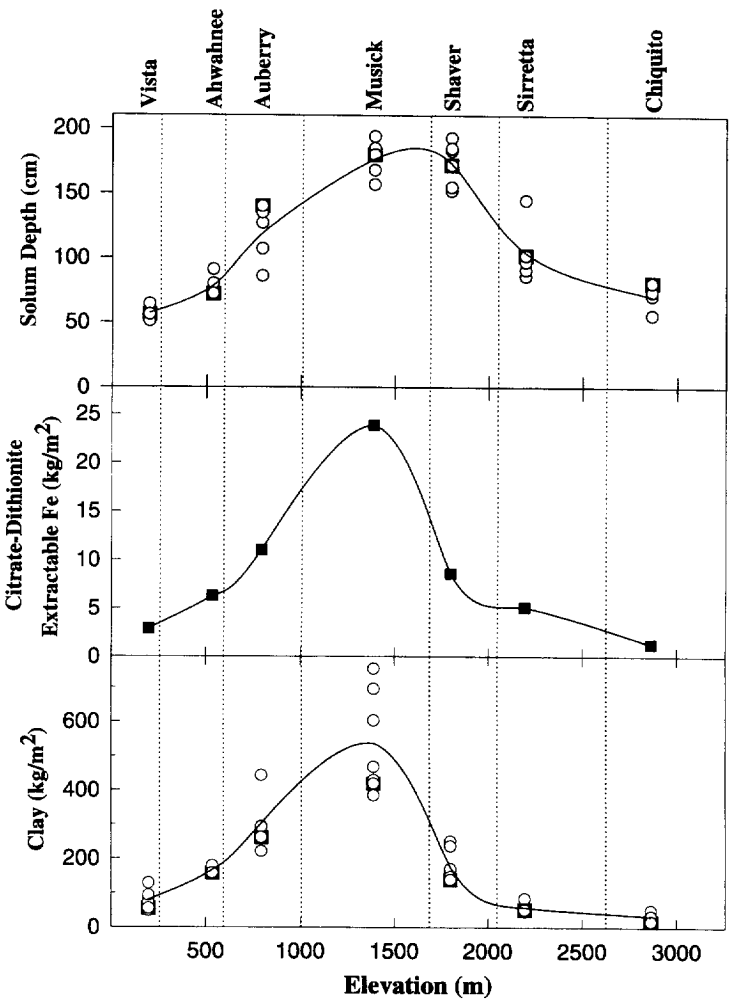

Fig. 10. Solum (A and B horizons) depth and solum concentrations of clay and secondary iron oxides (Fe_d) for the seven soils composing the elevational transect. Filled squares represent data analyzed in this study and circles represent data from soil survey characterization data ($n = 3–5$) in this area. The line represents the mean of all data points for each soil.

are near freezing when the soils are moist, possibly limiting the effects of water on physical weathering. Freeze–thaw cycle physical weathering may occur in the upper soil horizons during winter at lower and intermediate elevations and during the late fall in the high-elevation soils; however, the thick snowpack insulates these soils and prevents them from freezing during the winter.

The magnitude of chemical weathering along the elevational transect, indicated independently by clay and Fe_d concentrations in the solum, was greatest in the mid-elevation Musick soil (1390 m) (Fig. 10). Clay accumulation shows a maximum of

536 kg/m^2 at mid-elevations compared to 79 and 32 kg/m^2 at the lowest and highest elevation soils, respectively. Similarly, maximum Fe_d concentrations of 24 kg/m^2 were measured in the Musick soil decreasing to 3 and 2 kg/m^2 in the lowest and highest elevation soils, respectively. Assuming that these soils are near steady-state and of comparable age, these data indicate that weathering is most intense at intermediate levels of temperature (MAAT = 11.1°C) and precipitation (MAP = 91 cm). Weathering is limited primarily by cold soil temperatures at higher elevations and a lack of moisture at low elevations.

Previous studies of chemical weathering based on clay production (Jenny, 1941) and fluxes of weathering products (e.g., Na, Si) from watersheds (White and Blum, 1995) indicate that field rates of chemical weathering are an exponential function of temperature and a linear function of moisture (precipitation or leaching intensity). This would suggest that the degree of weathering should show a continuum as climatic factors change uniformly with elevation. The transition in soil properties between the Auberry (794 m) and the Musick (1390 m) soils changed gradually based on soil morphological features and the observed and mapped pattern of these soils. In contrast, the transition between the Musick (1390 m) and Shaver (1800 m) is very abrupt, occurring over a small elevational difference ($\sim$ 200 m). Solum concentrations of clay and Fe_d decrease by approximately 3-fold over the Musick to Shaver transition suggesting that the chemical weathering process is related to climate by a threshold function rather than a smooth continuum function.

3.7. Soil development response to climate

An observation that has intrigued soil scientists in California for many years is the abrupt transition in certain soil properties occurring between the Musick and Shaver soils at an elevation of approximately 1600 m. This observation is also valid for soils formed on parent materials other than granitic residuum in the central Sierra Nevada. While some soil properties show a continuous progression (e.g., organic carbon, base saturation, clay mineralogy) with elevation, other properties (e.g., soil color, clay and secondary iron concentrations, pH) show a pronounced change (threshold-type step) over very short horizontal (a few km) and elevational ($\sim$ 200 m) distances. The abrupt change coincides with the elevation of the present-day average effective winter snow-line (1594 m) (California Department of Water Resources, 1952–62). Above the winter snow-line, most of the precipitation falls in the form of snow and the snowpack melt and leaching occur primarily over a two-month period in the spring (April–June) when soil temperatures are near 0°C. In contrast, soils below the winter snow-line receive most of the precipitation as rainfall resulting in active leaching processes for approximately six months out of the year. While the data presented in this study cannot directly test this snow-line effect hypothesis, it does provide important evidence on which to base future studies.

This study indicates that soil properties and processes are strongly related to elevation and thus to climatic conditions. This suggests that shifts in climate will produce appreciable changes in soil properties resulting in a strong feedback to global biogeochemical cycles. The warmest Quaternary intervals were 2–3°C warmer than the present

climate (Goudie, 1983), which represents a 300–500 m elevation shift along our transect. Based on the transect, this temperature shift (with corresponding shift in precipitation) would result in a net loss of soil organic matter and no appreciable net change in rates of carbonic acid weathering. The loss of soil organic matter would result from the upward migration of the oak woodlands into the mixed-conifer zone. This loss may be partially compensated for by increased carbon storage in the high-elevation soils, especially those soils above the current-day tree line. While the zone of maximum weathering (Musick 1390 m) would move upward, this increase in weathering would be offset by lower weathering rates in the lower-elevation soils.

References

Alexander, E.B., Mallory, J.I., Colwell, W.L., 1993. Soil-elevation relationships on a volcanic plateau in the southern Cascade Range, northern California, USA. Catena 20, 113–128.

Allardice, W.R., Munn, S.S., Begg, E.L., Mallory, J.I., 1983. Laboratory data and descriptions for some typical pedons of California soils, Vol. 1. Central and Southern Sierra. Dept. of Land, Air and Water Resources, Univ. of California, Davis and Soil-Vegetation Survey, California Dept. of Forestry, Sacramento, CA.

Amundson, R.G., Chadwick, O.A., Sowers, J.M., 1989. A comparison of soil climate and biological activity along an elevation gradient in the eastern Mojave Desert. Oecologia 80, 395–400.

Anderson, R.S., 1990. Holocene forest development and paleoclimates within the central Sierra Nevada, California. J. Ecol. 78, 470–489.

Barnhisel, R.I., Bertsch, P.M., 1989. Chlorites and hydroxy-interlayered vermiculite and smectite. In: Dixon, J.B., Weed, S.B. (Eds.), Minerals in Soil Environments (2nd ed.). SSSA Book Series, 1, Madison, WI, pp. 729–788.

Barshad, I., 1966. The effect of a variation in precipitation on the nature of clay mineral formation in soils from acid and basic igneous rocks. Proc. Int. Clay Conf., Jerusalem 1, 167–173.

Bateman, P.C., Lockwood, J.P., 1970. Kaiser Peak Quadrangle, Central Sierra Nevada, California—Analytic Data. U.S. Geol. Surv. Prof. Pap. 644-C.

Bateman, P.C., Lockwood, J.P., 1976. Shaver Lake Quadrangle, Central Sierra Nevada, California—Analytic Data. U.S. Geol. Surv. Prof. Pap. 774-D.

Bateman, P.C., Wones, D.R., 1972. Huntington Lake Quadrangle, Central Sierra Nevada, California—Analytic Data. U.S. Geol. Surv. Prof. Pap. 724-A.

Beckett, P.H.T., Webster, R., 1971. Soil variability: a review. Soils Fert. 34, 1–15.

California Department of Water Resources, 1952–62. Water conditions in California. Bull. 120 Series, Sacramento, CA.

Childs, C.W., Parfitt, R.L., Lee, R., 1983. Movement of aluminum as an inorganic complex in some podzolised soils, New Zealand. Geoderma 29, 139–155.

Goudie, A., 1983. Environmental Change. Clarendon Press, Oxford, 257 pp.

Grieve, I.C., Proctor, J., Cousins, S.A., 1990. Soil variation with altitude on Volcan Barva, Costa Rica. Catena 17, 525–534.

Hanawalt, R.B., Whittaker, R.H., 1976. Altitudinally coordinated patterns of soils and vegetation in the San Jacinto Mountains, California. Soil Sci. 121, 114–124.

Harradine, F., Jenny, H., 1958. Influence of parent material and climate on texture and nitrogen and carbon contents of virgin California soils. Soil Sci. 85, 235–243.

Holmgren, G.G.S., 1967. A rapid citrate-dithionite extractable iron procedure. Soil Sci. Soc. Am. Proc. 31, 210–211.

Huntington, G.L., 1954. The effect of Vertical Zonality on Clay Content in Residual Granitic Soils of the Sierra Nevada Mountains. M.S. thesis, University of California, Berkeley.

Huntington, G.L., Akeson, M.A., 1987. Soil Resource Inventory of Sequoia National Park, Central Part, California. Univ. of California, Department of Land, Air and Water Resources, Davis, CA 95616.

Hsu, P.H., 1989. Aluminum hydroxides and oxyhydroxides. In: Dixon, J.B., Weed, S.B. (Eds.), Minerals in Soil Environments (2nd ed.). SSSA Book Series, 1, Madison, WI, pp. 331–378.

Iyengar, S.S., Zelazny, L.W., Martens, D.C., 1981. Effect of photolytic oxalate treatment on soil hydroxy-interlayered vermiculites. Clays Clay Miner. 29, 429–434.

Jenny, H., 1928. Relation of climatic factors to the amount of nitrogen in soils. J. Am. Soc. Agron. 20, 900–912.

Jenny, H., 1941. Factors of Soil Formation—A System of Quantitative Pedology. McGraw-Hill, New York, 281 pp.

Jenny, H., 1950. Causes of high nitrogen and organic matter content of certain tropical forest soils. Soil Sci. 69, 63–70.

Jenny, H., 1980. The Soil Resource. Springer-Verlag, New York, 377 pp.

Jenny, H., Gessel, S.P., Bingham, F.T., 1949. Comparative study of decomposition rates of organic matter in temperate and tropical regions. Soil Sci. 68, 419–432.

Karathanasis, A.D., 1988. Compositional and solubility relationships between aluminum-hydroxy interlayered soil—smectites and vermiculites. Soil Sci. Soc. Am. J. 52, 1500–1508.

Lavkulich, L.M., Wiens, J.H., 1970. Comparison of organic matter destruction by hydrogen peroxide and sodium hypochlorite and its effect on selected mineral constituents. Soil Sci. Soc. Am. Proc. 34, 755–758.

McKeague, J.A., 1967. An evaluation of 0.1 M pyrophosphate and pyrophosphate-dithionite in comparison with oxalate as extractants of accumulation products in podzols and some other soils. Can. J. Soil Sci. 47, 95–99.

McKeague, J.A. (Ed.), 1976. Manual on Soil Sampling and Methods of Analysis. Soil Researh Institute, Agriculture Canada, Ottawa.

Nettleton, W.D., Flach, K.W., Borst, G., 1968. A toposequence of soils in tonalite grus in the southern California Peninsular Range. Soil Surv. Invest. Rep. 21, USDA, Soil Conservation Service, Washington, D.C., 41 pp.

Parfitt, R.L., Childs, C.W., 1988. Estimation of forms of Fe and Al: A review, and analysis of contrasting soils by dissolution and Moessbauer methods. Aust. J. Soil Res. 26, 121–144.

Parfitt, R.L., Giltrap, D.J., Whitton, J.S., 1995. Contribution of organic matter and clay minerals to the cation exchange capacity of soils. Commun. Soil Sci. Plant Anal. 26, 1343–1355.

Ross, G.J., Kodama, H., Wang, C., Gray, J.T., Lafreniere, L.B., 1983. Halloysite from a strongly weathered soil at Mont Jacques Cartier, Quebec. Soil Sci. Soc. Am. J. 47, 327–332.

Schlesinger, W.H., 1991. Biogeochemistry—An Analysis of Global Change. Academic Press, New York, 443 pp.

Schwertmann, U., 1985. The effect of pedogenic environments on iron oxide minerals. Adv. Soil Sci. 1, 171–200.

Scuderi, L.A., 1993. A 2000-year tree ring record of annual temperatures in the Sierra Nevada Mountains. Science 259, 1433–1436.

Soil Conservation Service, 1994. National Soil Characterization Data. CD-ROM, National Soil Survey Center, Soil Survey Laboratory, Lincoln, NE.

Soil Survey Staff, 1981. Soil Survey Manual. USDA–SCS Agriculture Handbook, 18. U.S. Government Printing Office, Washington, D.C., 503 pp.

Soil Survey Staff, 1984. Procedures for collecting soil samples and methods of analysis for soil survey. Soil Surv. Invest. Rep. 1. USDA–SCS Agriculture Handbook, 436. U.S. Government Printing Office, Washington, D.C.

Soil Survey Staff, 1994. Keys to Soil Taxonomy (6th ed.). SMSS Technical Monograph, 19. Pocahontas Press, Blacksburg, VA.

Southard, R.J., Southard, S.B., 1987. Sand-sized kaolinized feldspar pseudomorphs in a California Humult. Soil Sci. Soc. Am. J. 51, 1666–1672.

Takahashi, T., Dahlgren, R.A., van Susteren, P., 1993. Clay mineralogy and chemistry of soils formed in volcanic materials in the xeric moisture regime of northern California. Geoderma 59, 131–150.

Tate, K.R., 1992. Assessment, based on a climosequence of soils in tussock grasslands, of soil carbon storage and release in response to global warming. J. Soil Sci. 43, 697–707.

Trumbore, S.E., Chadwick, O.A., Amundson, R., 1996. Rapid exchange between soil carbon and atmospheric carbon dioxide driven by temperature change. Science 272, 393–396.

Ulrich, B., 1980. Production and consumption of hydrogen ions in the ecosphere. In: Hutchinson, T.C., Havas, M. (Eds.), Effects of Acid Precipitation on Terrestrial Ecosystems. NATO Conference Series 1, part 4, Plenum Press, New York, pp. 255–282.

USDA California Forest and Range Experiment Station, 1955–1960. Soil-Vegetation Maps of California, Sierra National Forest, Fresno County. C.F. and R. Exp. Station in cooperation with Univ. of California, Berkeley and the U.S. Forest Service.

USDA Forest Service, 1986. Soil Survey of Sierra National Forest Area, California. U.S. Forest Service, 630 Sansome St., San Francisco, CA 94111.

USDA Soil Conservation Service, 1968. Soils of the Sierra Foothills, Vol. III, Published in cooperation with Fresno County General Plan Program. SCS, 2020 Milvia St., Berkeley, CA 94704.

Wada, K., Higashi, T., 1976. The categories of aluminum- and iron-humus complexes in Ando soils determined by selective dissolution. J. Soil Sci. 27, 357–368.

Wahrhaftig, C., 1965. Stepped topography of the southern Sierra Nevada, California. Geol. Soc. Am. Bull. 76, 1165–1190.

White, A.F., Blum, A.E., 1995. Effects of climate on chemical weathering in watersheds. Geochim. Cosmochim. Acta 59, 1729–1747.

Whittig, L.D., Allardice, W.R., 1986. X-ray diffraction techniques. In: Klute, A. (Ed.), Methods of Soil Analysis, Part 1. Physical and Mineralogical Methods. Agron. Monogr. 9 (2nd ed.). American Society of Agronomy, Madison, WI, pp. 331–362.

Yatsu, E., 1988. The Nature of Weathering—An Introduction. Sozosha, Tokyo, 624 pp.